ACS OMEGA

http://pubs.acs.org/journal/acsodf

Article

Highly Durable Superhydrophobic Polydimethylsiloxane/Silica Nanocomposite Surfaces with Good Self-Cleaning Ability

Xiao Gong* and Shuang He

Cite This: *ACS Omega* 2020, 5, 4100−4108

Read Online

ACCESS | Metrics & More | Article Recommendations | Supporting Information

ABSTRACT: In this work, we report that superhydrophobic coatings can be prepared by a simple spray-coating technique using readily available materials such as polydimethylsiloxane (PDMS) and hydrophilic and hydrophobic SiO_2 nanoparticles. PDMS can combine with the two kinds of SiO_2 nanoparticles to form a rough structure, which results in superhydrophobicity of the coatings. The prepared superhydrophobic coating has a water contact angle of 156.4° and a sliding angle of less than 5°. Moreover, the coatings can be applied to various substrates such as glass, paper, and plastic. In addition, the coatings show excellent stability and still remain superhydrophobic after ultraviolet radiation, sand abrasion and water impact, tape peeling, and treatment with a strong alkali/acid solution. Furthermore, the superhydrophobic surfaces are proven to be suitable for antifouling and self-cleaning.

1. INTRODUCTION

Recently, specially designed functional surfaces such as superhydrophobic surfaces, inspired by the "lotus effect" in nature, have attracted extensive attention because of their widespread application in materials science and engineering technology.[1−12] A superhydrophobic surface exhibits extremely high water resistance: the static contact angle of water is larger than 150° and the dynamic sliding angle is smaller than 10°.[13−15] Superhydrophobic surfaces are generally created by a micro−nanostructured rough surface and low-surface-energy material modification.[9,16−25] As water repellency is important in practical applications including self-cleaning,[26−28] oil−water separation,[29−37] corrosion protection,[38] and anti-icing,[39] there are a number of research works on superhydrophobic surfaces. For example, Ge et al.[40] reported that a transparent and superamphiphobic surface could be created from strings of amphiphilic silica nanoparticles dispersed in an amphiphilic sol solution by a one-step spray-coating method. Li et al.[41] fabricated a translucent and superhydrophobic polydimethylsiloxane (PDMS) coating on a glass substrate by introducing roughness using SiO_2 nanoparticles with an aerosol-assisted chemical vapor deposition method. Wu et al.[42] synthesized emulsions by a one-step method using nanoparticles, PTES, waterborne epoxy resin, and ethanol and prepared an environmentally friendly and stable superhydrophobic film by simply spraying them on the surface of a substrate. Although research on superhydrophobic surfaces has made significant progress, most preparation methods are still complicated, requiring special conditions and/or expensive equipment, which limit their practical application.

For superhydrophobic surfaces, high transparency is a requirement in many practical applications.[4,43−52] As we know, the transparency of coatings generally becomes worse when the surface roughness increases because light scattering occurs when light strikes the rough surface, causing the surface to exhibit translucence or opaqueness. Therefore, light scattering can be attenuated by reducing the roughness of the surface, making the surface transparent.[53] Previous studies on transparent and durable superhydrophobic surfaces were mainly related to carbon derivatives, polymers, and silicon nanoparticles.[54] Gao et al.[55] reported that a superhydrophobic surface could be obtained using PDMS as the binder, tetrahydrofuran as the solvent, and water as the nonsolvent by phase separation. Results showed that transmittance decreased by less than 10%. Alawajji et al.[56] successfully fabricated transparent superhydrophobic polytetrafluoroethylene thin films using pulsed laser deposition with various deposition times at room temperature, and the transmission rate could be as high as 90%. Unfortunately, although the desired hydrophobicity and transparency were obtained, the robustness and wear resistance of the film were not good because of the flexibility of the polymer.

In this paper, we present a simple, fast, and environmentally friendly one-step spray coating method for preparing superhydrophobic coatings on different substrates using readily available materials such as PDMS and SiO_2 nanoparticles. When hydrophilic SiO_2 and hydrophobic SiO_2 nanoparticles are mixed in a certain ratio and blended with PDMS, a roughly

Received: November 6, 2019
Accepted: January 23, 2020
Published: February 19, 2020

https://dx.doi.org/10.1021/acsomega.9b03775
ACS Omega 2020, 5, 4100−4108

hierarchical micro−nanostructured surface can be obtained, wherein PDMS is used as both a low surface energy modifier and an adhesive. After being exposed to ultraviolet (UV) light for 72 h, peeled off for 250 cycles by a tape, and immersed in a strong acid/base solution for 72 h, the superhydrophobic coatings still show good water resistance, revealing good durability. In addition, the coatings can maintain sufficient transparency, allowing them to be used in a wide range of applications. Based on their excellent superhydrophobicity and lipophilicity, the coatings can be used for large-scale applications in self-cleaning and oil−water separation.

2. EXPERIMENTAL WORK

2.1. Materials. PDMS was purchased from Toshiba Moto, Japan. Tetraethyl orthosilicate (TEOS) and hexane were purchased from Sinopharm Chemical Reagent Co., Ltd. Ditin butyl dilaurate ($C_{32}H_{64}O_4Sn$) and hydrophilic fumed nanosilica (7−40 nm) were purchased from Shanghai Macklin Biochemical Co., Ltd. Hydrophobic gas-phase nanosilica (7−40 nm) was purchased from Aladdin Biotechnology Corporation.

2.2. Preparation of Superhydrophobic Solution. First, a certain amount of PDMS was dissolved in 20 mL of *n*-hexane; an appropriate amount of TEOS and ditin butyl dilaurate (mass ratio of PDMS/TEOS was 10:1) was added, and ultrasonication was performed for several minutes. Subsequently, hydrophilic and hydrophobic silica were added to the solution in a certain ratio, and the total mass of the silica was maintained at 0.1 g. Finally, the solution was sonicated for 15 min.

2.3. Preparation of Superhydrophobic Films on Various Substrates by Spray-Coating. The glass substrate was repeatedly washed several times with deionized water and alcohol and dried in an oven. The prepared superhydrophobic suspension was spray-coated onto the surface of the substrates at a spray pressure of 5 psi for one cycle. Otherwise, the coating is too thick resulting in a decrease in transmittance. The prepared sample was placed in a room temperature environment for 1 h to obtain a superhydrophobic coating. In order to more clearly describe the prepared process, the complete process is shown in Figure 1a. As shown in Figure 1a, when PDMS and the curing agent are spray-coated on the substrate, the contact angle of the water droplets on the surface is only about 100°. Once hydrophilic nanosilica particles (red particles in Figure 1a) are added to the solvent, the nanoparticles may agglomerate because the surface of the hydrophilic nanoparticles has a hydroxyl group. Hydrophobic nanoparticles are continuously added to the solution, and the hydrophobic nanoparticles are not connected to the hydrophilic nanoparticles because the surface is modified. However, when PDMS is added to the nanoparticle solution, the hydrophobic nanoparticles are connected to the hydrophilic nanoparticles under the action of the adhesive PDMS. Eventually, the contact angle of the water droplets on the surface of the substrate can reach above 150°.

Fourier transform infrared (FTIR) spectra from 500 to 4000 cm^{-1} of hydrophilic and hydrophobic SiO_2@glass coatings are shown in Figure 1b. Hydrophobic nanoparticles are obtained by surface modification with hexamethyldisilazane (HMDS). At 3433 cm^{-1}, both hydrophilic and hydrophobic nano-SiO_2 have strong absorption peaks. The absorption peak at 3643 cm^{-1} reflects the stretching vibration of N−H bonds of the hydrophobic nanoparticles and the stretching vibration of the

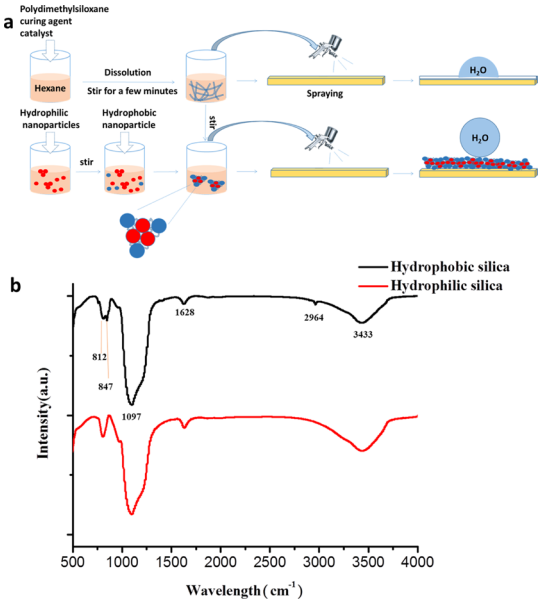

Figure 1. (a) Schematic of a process for preparing a superhydrophobic suspension and a semitransparent superhydrophobic coating. (b) FTIR spectra of hydrophilic and hydrophobic SiO_2.

hydroxyl groups of the hydrophilic nanoparticles. The absorption peak at 2964 cm^{-1} reflects the stretching vibration of Si−CH_3 of HMDS. A very high intensity absorption peak can be detected at 1097 cm^{-1} because of the asymmetric stretching of Si−O−Si. The absorption peaks at 812 and 847 cm^{-1} are derived from the stretching vibration of the Si−N bond in HMDS.

2.4. Characterization. The surface morphology of the coating was investigated by a JSM-IT300 field emission scanning electron microscope (FESEM). Elemental analysis was obtained from an energy dispersive spectroscopy (EDS) device connected to the FESEM. Infrared spectra of the substrates before and after coating were recorded using a Nicolet 6700 FTIR spectrometer. The static contact angle and sliding angle of the droplets were measured using a contact angle meter (Theta Lite, Biolin Scientific), and the volume of each droplet was 2 μL. A Shimadzu ultraviolet−visible near infrared spectrophotometer was used to measure the optical transmittance of the coating.

2.5. Durability Testing. In order to study the durability of the prepared superhydrophobic coatings, various experiments were conducted including the tape peeling test, the UV resistance test, and the corrosion resistance test. The static contact angle and the sliding angle were recorded to show that the coating remained superhydrophobic. The tape peeling test was conducted using an ordinary tape to investigate the adhesion between the superhydrophobic coating and the substrate, and the contact angle and sliding angle were measured every 50 cycles. In order to study the aging resistance of the sample under UV irradiation, the sample was exposed to UV light for 72 h, and the contact angle and sliding angle were recorded every 12 h. The corrosion resistance test was carried out by immersing the superhydrophobic coatings in hydrochloric acid or sodium hydroxide solution (pH from 1 to 14) for 72 h, and then the contact angle and sliding angle of the soaked samples were measured.

2.6. Self-Cleaning Ability. In order to prove the self-cleaning property of the prepared superhydrophobic films,

https://dx.doi.org/10.1021/acsomega.9b03775
ACS Omega 2020, 5, 4100−4108

black carbon powder was selected as the model dust and put on the surface of the film. The superhydrophobic film was tilted with a certain angle in a Petri dish. Then, water droplets were dropped on the superhydrophobic film. The water droplets could pick up and remove the toner.

2.7. Sand Drop Abrasion and Water Drop Impact. During the sand drop abrasion test, 10, 30, and 50 g of sand particles with a particle size of about 0.4 mm were dropped from a height of 50 cm and impinged on the superhydrophobic coating for 30 s. In the water droplet impact experiment, at a height of 50 cm above the superhydrophobic coating, 5,000 water droplets (~2 μL each) were dropped, and the contact angle of the hydrophobic layer was recorded.

3. RESULTS AND DISCUSSION

Figure 2a illustrates the preparation of a superhydrophobic surface by a simple spray-coating method. As shown in Figure 2b, the prepared superhydrophobic coatings could be applied to different substrates such as glass, plastic, and paper. In order to create a suitable micro−nano structure, we studied the effect of different ratios of hydrophilic SiO_2 to hydrophobic SiO_2 on the surface structure of the coatings. Figure 3 shows the typical scanning electron microscopy (SEM) images of coatings with different ratios of hydrophilic SiO_2 to hydrophobic SiO_2. The results showed that the ratio of hydrophilic SiO_2 to hydrophobic SiO_2 had a great influence on the surface structure of the coating. When the ratio was 1:5, nanoparticles aggregated to form many small clusters, and the size of the clusters was small (Figure 3a). As the fraction of hydrophilic nano-SiO_2 increased, nanoparticles began to aggregate to form irregularly big clusters. Once the ratio was 4:2, the amount of nanoparticles and the size of clusters deposited on the glass surface increased dramatically (Figure 3c). However, when the fraction of hydrophilic SiO_2 further increased and reached 5:1, the amount of nanoparticles and the size of clusters became small again (Figure 3d). Figure 3e shows the typical EDS spectrum and the elemental ratio of the coating. The surface mainly contained C, O, and Si elements, and the atomic ratios were 0.4, 43.73, and 55.86%, respectively. The content of Si significantly increased compared to that of pristine glass.

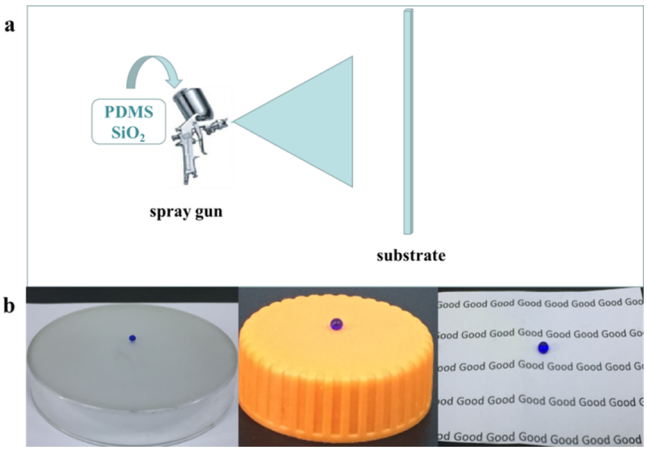

Figure 2. (a) Schematic illustration of superhydrophobic preparation. (b) Water droplets on superhydrophobic coatings applied to various substrates.

In order to investigate the relationship between the amount of PDMS and the superhydrophobicity of the coating, 0.5, 1.0, 1.5, and 2.0 g of PDMS were added to the solutions containing 0.1 g of SiO_2 nanoparticles (the ratio of hydrophilic SiO_2 to hydrophobic SiO_2 was 1:1). It could be seen from the SEM image that when the amount of PDMS was 0.5 g, nanoparticles on the surface of the glass substrate aggregated and the cluster size became large (Figure 4a). The coating showed significant superhydrophobicity. However, as the amount of PDMS increased (e.g., 1.5 g), although the amount of nanoparticles on the substrate surface did not reduce, the surface of the particles was covered by PDMS and became smooth. The coating lost superhydrophobicity (Figure 4c). The morphology difference between the blank glass and the superhydrophobic coating surface could be seen from the SEM images (Figure S1).

Figure 4e shows the FTIR plots of PDMS@glass coating and PDMS/hydrophilic and hydrophobic SiO_2@glass coatings from 500 to 4000 cm^{-1}. Results proved that SiO_2 and PDMS could be connected together. The absorption peaks at 2965 and 1263 cm^{-1} reflected the asymmetric stretching and deformation of CH_3 in Si−CH_3 of PDMS. The absorption peaks at 806 and 799 cm^{-1} represented the Si−$(CH_3)_2$ stretching vibration of PDMS. A very high intensity absorption peak could be detected at 1019 cm^{-1}, which was ascribed to the asymmetric stretching of Si−O−Si. The absorption peak at 865 cm^{-1} proved that PDMS and SiO_2 were completely connected.

It is well known that the hydrophobicity of a coating depends on its surface topography and surface energy. In this work, we used hydrophobic and hydrophilic silica nanoparticles to create high surface roughness and used PDMS as a low-surface-energy agent and an adhesive to prepare superhydrophobic coatings. In order to investigate the relationship between the wettability of the surface coating (contact angle and sliding angle) and the preparing conditions (the ratio of hydrophilic to hydrophobic silica nanoparticles to the amount of PDMS), we carried out a series of experiments. As shown in Figure 5a, when the amount of PDMS was 1 g and the total amount of silica was 0.1 g, as the proportion of hydrophobic silica increased, the water contact angle increased first and then decreased. However, the sliding angle first decreased and then increased. When the ratio of hydrophilic to hydrophobic silica was 4:2 and 3:3, the coating showed good superhydrophobicity. However, the coating had a water contact angle lower than 150° and a sliding angle larger than 10° in other ratios; even when the ratio of hydrophilic to hydrophobic SiO_2 was 1:5 and 0:6, the sliding angle was larger than 50°. This is because the surface roughness of the coating is not high enough under these conditions.

In addition, we also studied the effect of the amount of PDMS on the wettability of the coating when the total amount of hydrophilic and hydrophobic silica was 0.1 g and the ratio was 3:3. It can be seen from Figure 5c that as the amount of PDMS increased, the contact angle of the coating decreased and the sliding angle increased. When the amount of PDMS was 0.5 and 1 g, the contact angle of the coating was larger than 150° and the sliding angle was lower than 5°. Under this condition, the coating showed obvious superhydrophobicity. However, as the amount of PDMS increased, the hydrophobicity of the coating gradually decreased. When the amount of PDMS reached 1.5 g, the contact angle of the coating was lower than 150° and the sliding angle was larger than 10°, revealing that the coating lost superhydrophobicity. This is because as the amount of PDMS increases, more PDMS covers

https://dx.doi.org/10.1021/acsomega.9b03775
ACS Omega 2020, 5, 4100−4108

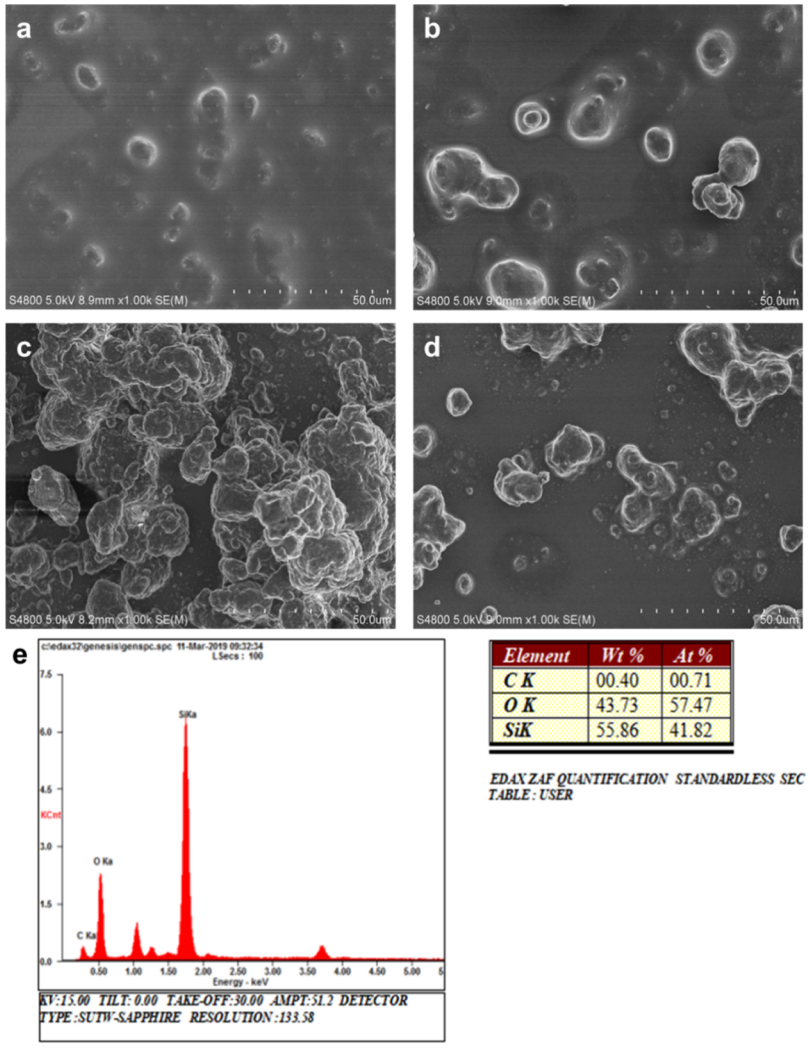

Figure 3. SEM images of hydrophilic SiO_2/hydrophobic SiO_2 = (a) 1:5, (b) 2:4, (c) 4:2, and (d) 5:1. (e) EDS spectrum and elemental ratio of a coating.

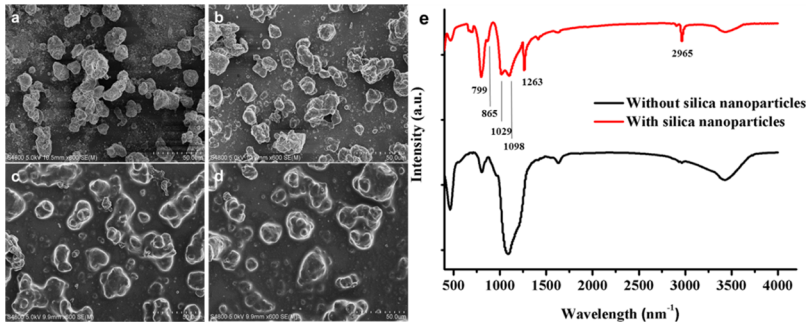

Figure 4. SEM images of the amount of (a) 0.5, (b) 1, (c) 1.5, and (d) 2.0 g of PDMS. (e) FTIR diagram of PDMS@glass and PDMS/hydrophilic and hydrophobic SiO_2.

the surface of the nanoparticles, reducing the surface roughness. According to the previous report, hydrophilic silica nanoparticles possess many OH^- groups which cause nanoparticles to aggregate,[57] whereas hydrophobic silica nanoparticles contain many hydrophobic groups which make nanoparticles disperse better. Thus, the appropriate ratio of hydrophobic nanoparticles to hydrophilic nanoparticles will cause hydrophilic nanoparticles to form appropriate microstructured aggregation, which can create a good rough surface, resulting in a superhydrophobic surface.

The transmittance of the sample prepared was measured. Blank glass had an approximate 92% visible light transmission. It can be seen from Figure 5b that as the ratio of hydrophilic to hydrophobic nanoparticles was fixed and the amount of PDMS increased, the transmittance of the coating increased in the wavelength range from 400 to 800 nm. When the amount of PDMS was 2.0 g, the coating transmittance at this time was the

https://dx.doi.org/10.1021/acsomega.9b03775
ACS Omega 2020, 5, 4100−4108

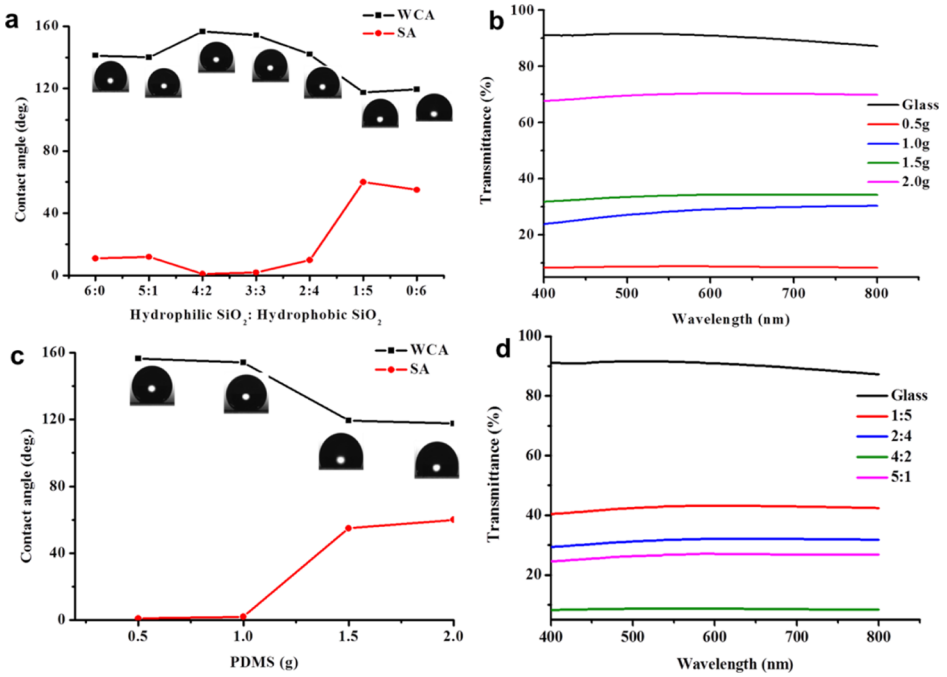

Figure 5. Relationship of contact angles and sliding angles with (a) the ratio of SiO_2 nanoparticles and (c) the amount of PDMS. (b) Relationship between transparency and PDMS amount in the nanoparticle ratio of 3:3. (d) Relationship between transparency and nanoparticle ratio when the amount of PDMS was 1 g.

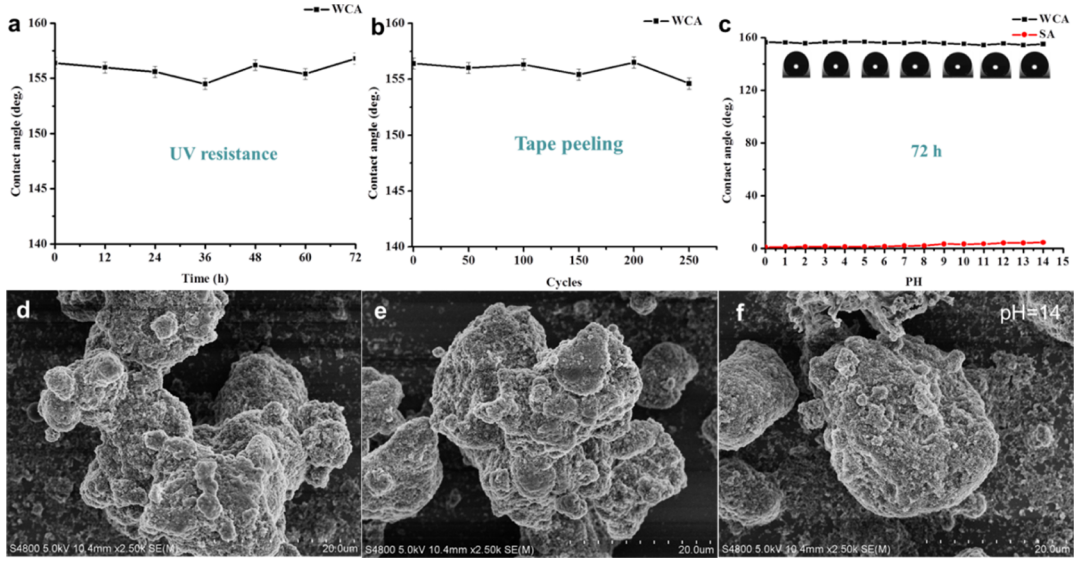

Figure 6. Contact angle of superhydrophobic coating prepared after UV irradiation (nanoparticle ratio was 4:2, and the amount of PDMS was 1 g) for (a) various times and (b) tape peeling for different cycles. (c) Changes in the contact angle and sliding angle when the superhydrophobic film was immersed in hydrochloric acid solution or sodium hydroxide solution (pH = 1−14) for 72 h; SEM image (d) after tape peeling for 250 cycles and (e,f) for samples immersed in HCl solution (pH = 2) and NaOH solution (pH = 14) for 72 h.

highest (about 70%). Once the amount of PDMS decreased to 0.5 g, the visible light transmittance of the coating was less than 10%. However, at this time, the coating exhibited the most hydrophobicity. When the amount of PDMS reduced to 1 g, the coating at this time showed superhydrophobicity, but the transmittance reduced to 40%. The transmittance of the coating was also studied in different ratios of hydrophilic to hydrophobic nanoparticles. In general, superhydrophobicity and transparency are in a competitive relationship depending on the thickness and surface structure of the coating. As shown in Figure 5d, when the ratio was 1:5, the coating had the highest transmittance. When the ratio increased to 4:2, the coating had the best hydrophobicity, but the transmittance was less than 10%. This is because when the ratio of hydrophilic SiO_2 to hydrophobic SiO_2 was 4:2, the surface roughness of the coating reached the maximum value at this time. The results of the transparency test were comparable to SEM, contact angle, and sliding angle tests.

The mechanical instability of the superhydrophobic coatings is the main factor limiting their practical application. Here, we studied the stability of the coating by exposing it to UV light, peeling it off by a tape, and immersing it in a corrosive solution

https://dx.doi.org/10.1021/acsomega.9b03775
ACS Omega 2020, 5, 4100−4108

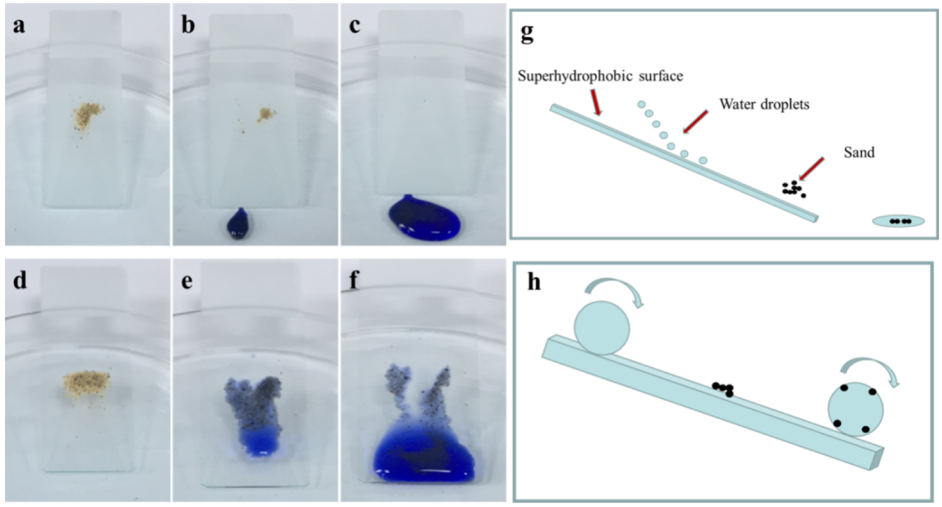

Figure 7. Self-cleaning process of (a−c) superhydrophobic coating and (d−f) blank glass. (g,h) Corresponding schematic illustration of the self-cleaning process.

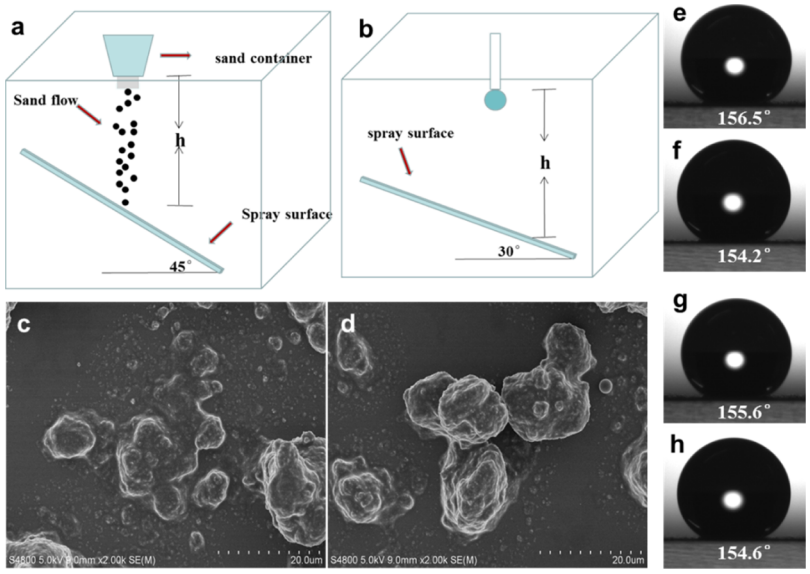

Figure 8. (a) Sketch of the setup for sand abrasion test; (b) schematic diagram of the setup for water droplet impact test; (c) SEM image of the superhydrophobic surface after the sand abrasion test with 50 g sand; (d) SEM image of the superhydrophobic surface after the water droplet impact test; water droplet contact angle after sand abrasion with (e) 10, (f) 30, and (g) 50 g; (h) contact angle after water droplet impact.

(strong acid/base). As shown in Figure 6a, after the prepared superhydrophobic coating (the mass ratio of hydrophilic SiO_2 to hydrophobic SiO_2 was 4:2, and the amount of PDMS was 1 g) was exposed to UV light for 72 h, there was no significant change in the hydrophobicity of the coating during the entire UV light irradiation, and the coating still kept good superhydrophobicity. This should be attributed to the fact that both PDMS and SiO_2 have excellent UV stability and are not easily degraded under UV irradiation. Moreover, we tested the adhesion of the coating to the substrate by repeatedly applying an adhesive tape to the surface of the coating. It can be seen that after being peeled off 250 times, the contact angle of the coating did not change substantially throughout the experiment, the contact angle of the coating was always larger than 150°, and the coating remained superhydrophobic (Figure 6b). In addition, it can be seen from the SEM image (Figure 6d) that the surface structure of the coating was not destroyed after 250 times of tape peeling, which proved the good stability of the coating.

Corrosion test was carried out by immersing the prepared superhydrophobic coating samples (hydrophilic SiO_2/hydrophobic SiO_2 = 4:2, PDMS was 1 g) into a hydrochloric acid or sodium hydroxide solution (pH from 1 to 14) for 72 h. As can be seen from Figure 6c, the effect on the coating was relatively small. The contact angle of the coating was still larger than 150°; but when the pH reached 12−14, the contact angle of the coating decreased slightly. From the SEM image (Figure 7e,f), we could see that the coating had no obvious change in the surface morphology after being treated in a solution of pH = 2 and pH = 14 for 72 h, respectively. This may be because the superhydrophobicity of the coating surface prevents the corrosive solution from contacting with the surface of the coating, so the surface layer of the coating is not corroded.

Water resistance is one of the most important properties of superhydrophobic coatings (Figure S2); the self-cleaning

https://dx.doi.org/10.1021/acsomega.9b03775
ACS Omega 2020, 5, 4100−4108

performance can effectively make the substrate (such as glass and plastic) automatically keep the surface clean with rain. Here, the self-cleaning properties of superhydrophobic coatings were studied using sand particles with a particle size of 0.4 mm as a model pollutant/dust. As shown in Figure 7a−c, some sand was deposited on a glass-based superhydrophobic coating. Water droplets were stained with methyl blue for comparison. During the self-cleaning process, the water droplets could pick up and remove the sand when rolling off the superhydrophobic surface because of superhydrophobicity and a small sliding angle, leaving a clean surface (Figure 7g,h). In contrast, when the uncoated glass was subjected to the same treatment (Figure 7d−f), the surface clearly retained traces of water droplets, and the sand slid with the water droplets which made the surface dirtier.

Mechanical durability is a key issue for the application of superhydrophobic coatings in practice. However, for superhydrophobic coatings, it is necessary to create a rough structure on the surface. However, the roughness can be easily destroyed during the wear process, resulting in poor durability of the coating. In recent studies, sand abrasion and water drop impact tests are often used to test the mechanical durability of coatings on substrates. The experiments on sand abrasion depend mainly on the quality and height of the sand. In our case (Figure 8a), 10, 30, and 50 g of sand grains with an average particle size of 0.4 mm were naturally dropped at a height of 50 cm, and the sand hit the superhydrophobic surface for 30 s. The surface morphologies of the surface after 10 g and 30 g sand abrasion were checked with SEM images (Figure S3). Even after the coating was hit by 50 g of sand grains, the microstructure of the surface was not destroyed (Figure 8c). Therefore, there was almost no change in the contact angle of the coating (Figure 8e−g). The coating still showed superhydrophobicity.

In the water drop impact test (Figure 8b), approximately 5000 water droplets were dropped from 50 cm above the coating for 2 h to test the stability of the coating. After the impact of water droplets, the coating still showed good superhydrophobicity (Figure 8h). According to the SEM image after water impact (Figure 8d), we could see that the surface structure almost did not change, revealing good water impact resistance. In order to study the effect of PDMS on the wear resistance of the coating, the same test was carried out on the coating entirely consisting of SiO_2. From the SEM image (Figure S4), it could be found that in the absence of PDMS, the surface structures after sand abrasion and water impact were severely damaged and the contact angle was greatly reduced, indicating that PDMS enhances the stability and hydrophobicity of the coating.

4. CONCLUSIONS

In summary, we successfully fabricated semitransparent and stable superhydrophobic coatings on various substrates such as glass, plastic, and paper. In the preparation process, we prepared the coatings by simple environmentally friendly materials with a spray-coating method. The rough structure with a low surface energy made these coatings excellent superhydrophobic with a water contact angle of 156.4° and a sliding angle of lower than 5°. After the coatings were subjected to UV radiation, tape peeling, sand abrasion, water droplet impact, and strong acid/base corrosion, they still exhibited good superhydrophobicity. In addition, glass-based superhydrophobic coatings endowed them good transparency. The prepared superhydrophobic surface had a low adhesion to water, and the water droplets could easily roll off from a slightly titled surface. Based on the above characteristics, this technology is expected to be used in the fields of engineering materials, self-cleaning glass, oil−water separation, corrosion protection, and so on.

■ ASSOCIATED CONTENT

Supporting Information

The Supporting Information is available free of charge at https://pubs.acs.org/doi/10.1021/acsomega.9b03775.

SEM images of blank glass and the prepared superhydrophobic coating, photographs of the spray-coated paper and uncoated paper immersed in water and then taken out of water, SEM images of the superhydrophobic surfaces after the sand abrasion test, and SEM images of the SiO_2 nanoparticle coating without PDMS after water droplet impact and sand abrasion impact (PDF)

■ AUTHOR INFORMATION

Corresponding Author

Xiao Gong − *State Key Laboratory of Silicate Materials for Architectures, Wuhan University of Technology, Wuhan 430070, China; State Key Laboratory of Polymer Materials Engineering, Sichuan University, Chengdu 610065, China;* orcid.org/0000-0002-5513-5354; Email: xgong@whut.edu.cn

Author

Shuang He − *State Key Laboratory of Silicate Materials for Architectures, Wuhan University of Technology, Wuhan 430070, China*

Complete contact information is available at: https://pubs.acs.org/10.1021/acsomega.9b03775

Notes

The authors declare no competing financial interest.

■ ACKNOWLEDGMENTS

This work was supported by the National Natural Science Foundation of China (no. 21774098) and the Open Foundation of the State Key Laboratory of Silicate Materials for Architectures at WUT (no. SYSJJ2018-04). This study is also financially supported by the Opening Project of State Key Laboratory of Polymer Materials Engineering (Sichuan University) (grant no. sklpme2019-4-26).

■ REFERENCES

(1) Wang, S.; Liu, K.; Yao, X.; Jiang, L. Bioinspired Surfaces with Superwettability: New Insight on Theory, Design, and Applications. *Chem. Rev.* **2015**, *115*, 8230−8293.

(2) Neinhuis, C.; Barthlott, W. Characterization and Distribution of Water-repellent, Self-cleaning Plant Surfaces. *Ann. Bot.* **1997**, *79*, 667−677.

(3) Nakajima, A.; Fujishima, A.; Hashimoto, K.; Watanabe, T. Preparation of Transparent Superhydrophobic Boehmite and Silica Films by Sublimation of Aluminum Acetylacetonate. *Adv. Mater.* **1999**, *11*, 1365−1368.

(4) Deng, X.; Mammen, L.; Butt, H.-J.; Vollmer, D. Candle soot as a template for a transparent robust superamphiphobic coating. *Science* **2012**, *335*, 67−70.

(5) Bellanger, H.; Darmanin, T.; Taffin de Givenchy, E.; Guittard, F. Chemical and physical pathways for the preparation of superoleophobic surfaces and related wetting theories. *Chem. Rev.* **2014**, *114*, 2694−2716.
(6) Liu, K.; Jiang, L. Bio-inspired design of multiscale structures for function integration. *Nano Today* **2011**, *6*, 155−175.
(7) Cao, M.; Li, K.; Dong, Z.; Yu, C.; Yang, S.; Song, C.; Liu, K.; Jiang, L. Superhydrophobic ″Pump″: Continuous and Spontaneous Antigravity Water Delivery. *Adv. Funct. Mater.* **2015**, *25*, 4114−4119.
(8) Li, S.; Huang, J.; Chen, Z.; Chen, G.; Lai, Y. A review on special wettability textiles: theoretical models, fabrication technologies and multifunctional applications. *J. Mater. Chem. A* **2017**, *5*, 31−55.
(9) Zhou, H.; Wang, H.; Niu, H.; Gestos, A.; Wang, X.; Lin, T. Fluoroalkyl silane modified silicone rubber/nanoparticle composite: a super durable, robust superhydrophobic fabric coating. *Adv. Mater.* **2012**, *24*, 2409−2412.
(10) Zhou, H.; Wang, H.; Niu, H.; Gestos, A.; Lin, T. Robust, Self-Healing Superamphiphobic Fabrics Prepared by Two-Step Coating of Fluoro-Containing Polymer, Fluoroalkyl Silane, and Modified Silica Nanoparticles. *Adv. Funct. Mater.* **2013**, *23*, 1664−1670.
(11) Gao, S.; Tang, G.; Hua, D.; Xiong, R.; Han, J.; Jiang, S.; Zhang, Q.; Huang, C. Stimuli-responsive bio-based polymeric systems and their applications. *J. Mater. Chem. B* **2019**, *7*, 709−729.
(12) Li, J.; Xu, C.; Zhang, Y.; Wang, R.; Zha, F.; She, H. Robust superhydrophobic attapulgite coated polyurethane sponge for efficient immiscible oil/water mixture and emulsion separation. *J. Mater. Chem. A* **2016**, *4*, 15546−15553.
(13) Wang, Y.; Gong, X. Special oleophobic and hydrophilic surfaces: approaches, mechanisms, and applications. *J. Mater. Chem. A* **2017**, *5*, 3759−3773.
(14) Wang, Y.; Gong, X. Superhydrophobic Coatings with Periodic Ring Structured Patterns for Self-Cleaning and Oil-Water Separation. *Adv. Mater. Interfaces* **2017**, *4*, 1700190.
(15) Zhong, L.; Gong, X. Phase separation-induced superhydrophobic polylactic acid films. *Soft Matter* **2019**, *15*, 9500−9506.
(16) Chen, L.; Guo, Z.; Liu, W. Outmatching superhydrophobicity: bio-inspired re-entrant curvature for mighty superamphiphobicity in air. *J. Mater. Chem. A* **2017**, *5*, 14480−14507.
(17) Yong, J.; Chen, F.; Yang, Q.; Du, G.; Shan, C.; Bian, H.; Farooq, U.; Hou, X. Bioinspired transparent underwater superoleophobic and anti-oil surfaces. *J. Mater. Chem. A* **2015**, *3*, 9379−9384.
(18) Cao, C.; Ge, M.; Huang, J.; Li, S.; Deng, S.; Zhang, S.; Chen, Z.; Zhang, K.; Al-Deyab, S. S.; Lai, Y. Robust fluorine-free superhydrophobic PDMS-ormosil@fabrics for highly effective self-cleaning and efficient oil-water separation. *J. Mater. Chem. A* **2016**, *4*, 12179−12187.
(19) Liu, H.; Wang, Y.; Huang, J.; Chen, Z.; Chen, G.; Lai, Y. Bioinspired Surfaces with Superamphiphobic Properties: Concepts, Synthesis, and Applications. *Adv. Funct. Mater.* **2018**, *28*, 1707415.
(20) Zhang, S.; Huang, J.; Tang, Y.; Li, S.; Ge, M.; Chen, Z.; Zhang, K.; Lai, Y. Understanding the Role of Dynamic Wettability for Condensate Microdrop Self-Propelling Based on Designed Superhydrophobic TiO2Nanostructures. *Small* **2017**, *13*, 1600687.
(21) Gong, G.; Gao, K.; Wu, J.; Sun, N.; Zhou, C.; Zhao, Y.; Jiang, L. A highly durable silica/polyimide superhydrophobic nanocomposite film with excellent thermal stability and abrasion-resistant performance. *J. Mater. Chem. A* **2015**, *3*, 713−718.
(22) Su, B.; Tian, Y.; Jiang, L. Bioinspired Interfaces with Superwettability: From Materials to Chemistry. *J. Am. Chem. Soc.* **2016**, *138*, 1727−1748.
(23) Wang, L.; Gao, C.; Hou, Y.; Zheng, Y.; Jiang, L. Magnetic field-guided directional rebound of a droplet on a superhydrophobic flexible needle surface. *J. Mater. Chem. A* **2016**, *4*, 18289−18293.
(24) Li, N.; Wu, L.; Yu, C.; Dai, H.; Wang, T.; Dong, Z.; Jiang, L. Ballistic Jumping Drops on Superhydrophobic Surfaces via Electrostatic Manipulation. *Adv. Mater.* **2018**, *30*, 1703838.
(25) Lv, D.; Wang, R.; Tang, G.; Mou, Z.; Lei, J.; Han, J.; De Smedt, S.; Xiong, R.; Huang, C. Ecofriendly Electrospun Membranes Loaded with Visible-Light-Responding Nanoparticles for Multifunctional Usages: Highly Efficient Air Filtration, Dye Scavenging, and Bactericidal Activity. *ACS Appl. Mater. Interfaces* **2019**, *11*, 12880−12889.
(26) Hong, D.; Bae, K.; Hong, S.-P.; Park, J. H.; Choi, I. S.; Cho, W. K. Mussel-inspired, perfluorinated polydopamine for self-cleaning coating on various substrates. *Chem. Commun.* **2014**, *50*, 11649−11652.
(27) Yoon, H.; Kim, H.; Latthe, S. S.; Kim, M.-w.; Al-Deyab, S.; Yoon, S. S. A highly transparent self-cleaning superhydrophobic surface by organosilane-coated alumina particles deposited via electrospraying. *J. Mater. Chem. A* **2015**, *3*, 11403−11410.
(28) Peng, J.; Zhao, X.; Wang, W.; Gong, X. Durable Self-Cleaning Surfaces with Superhydrophobic and Highly Oleophobic Properties. *Langmuir* **2019**, *35*, 8404−8412.
(29) Ma, W.; Zhang, M.; Liu, Z.; Kang, M.; Huang, C.; Fu, G. Fabrication of highly durable and robust superhydrophobic-superoleophilic nanofibrous membranes based on a fluorine-free system for efficient oil/water separation. *J. Membr. Sci.* **2019**, *570−571*, 303−313.
(30) Ma, W.; Zhang, M.; Liu, Z.; Huang, C.; Fu, G. Nature-inspired creation of a robust free-standing electrospun nanofibrous membrane for efficient oil-water separation. *Environ. Sci. Nano* **2018**, *5*, 2909−2920.
(31) Ma, W.; Zhao, J.; Oderinde, O.; Han, J.; Liu, Z.; Gao, B.; Xiong, R.; Zhang, Q.; Jiang, S.; Huang, C. Durable superhydrophobic and superoleophilic electrospun nanofibrous membrane for oil-water emulsion separation. *J. Colloid Interf. Sci.* **2018**, *532*, 12−23.
(32) Ma, W.; Samal, S. K.; Liu, Z.; Xiong, R.; De Smedt, S. C.; Bhushan, B.; Zhang, Q.; Huang, C. Dual pH- and ammonia-vapor-responsive electrospun nanofibrous membranes for oil-water separations. *J. Membr. Sci.* **2017**, *537*, 128−139.
(33) Ma, W.; Guo, Z.; Zhao, J.; Yu, Q.; Wang, F.; Han, J.; Pan, H.; Yao, J.; Zhang, Q.; Samal, S. K.; De Smedt, S. C.; Huang, C. Polyimide/cellulose acetate core/shell electrospun fibrous membranes for oil-water separation. *Sep. Purif. Technol.* **2017**, *177*, 71−85.
(34) Ma, W.; Zhang, Q.; Samal, S. K.; Wang, F.; Gao, B.; Pan, H.; Xu, H.; Yao, J.; Zhan, X.; De Smedt, S. C.; Huang, C. Core-sheath structured electrospun nanofibrous membranes for oil-water separation. *RSC Adv.* **2016**, *6*, 41861−41870.
(35) Li, J.; Xu, C.; Guo, C.; Tian, H.; Zha, F.; Guo, L. Underoil superhydrophilic desert sand layer for efficient gravity-directed water-in-oil emulsions separation with high flux. *J. Mater. Chem. A* **2018**, *6*, 223−230.
(36) Long, Y.; Shen, Y.; Tian, H.; Yang, Y.; Feng, H.; Li, J. Superwettable Coprinus comatus coated membranes used toward the controllable separation of emulsified oil/water mixtures. *J. Membr. Sci.* **2018**, *565*, 85−94.
(37) Zhang, M.; Ma, W.; Cui, J.; Wu, S.; Han, J.; Zou, Y.; Huang, C. Hydrothermal synthesized UV-resistance and transparent coating composited superoloephilic electrospun membrane for high efficiency oily wastewater treatment. *J. Hazard. Mater.* **2020**, *383*, 121152.
(38) Isimjan, T. T.; Wang, T.; Rohani, S. A novel method to prepare superhydrophobic, UV resistance and anti-corrosion steel surface. *Chem. Eng. J.* **2012**, *210*, 182−187.
(39) Tang, Y.; Zhang, Q.; Zhan, X.; Chen, F. Superhydrophobic and anti-icing properties at overcooled temperature of a fluorinated hybrid surface prepared via a sol-gel process. *Soft Matter* **2015**, *11*, 4540−4550.
(40) Ge, D.; Yang, L.; Zhang, Y.; Rahmawan, Y.; Yang, S. Transparent and Superamphiphobic Surfaces from One-Step Spray Coating of Stringed Silica Nanoparticle/Sol Solutions. *Part. Part. Syst. Charact.* **2014**, *31*, 763−770.
(41) Zhong, M.; Zhang, Y.; Li, X.; Wu, X. Facile fabrication of durable superhydrophobic silica/epoxy resin coatings with compatible transparency and stability. *Surf. Coat. Tech.* **2018**, *347*, 191−198.
(42) Wu, Y.; Jia, S.; Wang, S.; Qing, Y.; Yan, N.; Wang, Q.; Meng, T. A facile and novel emulsion for efficient and convenient fabrication of

https://dx.doi.org/10.1021/acsomega.9b03775
ACS Omega 2020, 5, 4100−4108

durable superhydrophobic materials. *Chem. Eng. J.* **2017**, *328*, 186−196.
(43) Deng, X.; Mammen, L.; Zhao, Y.; Lellig, P.; Müllen, K.; Li, C.; Butt, H.-J.; Vollmer, D. Transparent, thermally stable and mechanically robust superhydrophobic surfaces made from porous silica capsules. *Adv. Mater.* **2011**, *23*, 2962−2965.
(44) Han, J. T.; Kim, S. Y.; Woo, J. S.; Lee, G.-W. Transparent, Conductive, and Superhydrophobic Films from Stabilized Carbon Nanotube/Silane Sol Mixture Solution. *Adv. Mater.* **2008**, *20*, 3724−3727.
(45) Chun, D.-M.; Davaasuren, G.; Ngo, C.-V.; Kim, C.-S.; Lee, G.-Y.; Ahn, S.-H. Fabrication of transparent superhydrophobic surface on thermoplastic polymer using laser beam machining and compression molding for mass production. *CIRP Ann.* **2014**, *63*, 525−528.
(46) Davaasuren, G.; Ngo, C.-V.; Oh, H.-S.; Chun, D.-M. Geometric study of transparent superhydrophobic surfaces of molded and grid patterned polydimethylsiloxane (PDMS). *Appl. Surf. Sci.* **2014**, *314*, 530−536.
(47) Huang, W.-H.; Lin, C.-S. Robust superhydrophobic transparent coatings fabricated by a low-temperature sol-gel process. *Appl. Surf. Sci.* **2014**, *305*, 702−709.
(48) Vakarelski, I. U.; Patankar, N. A.; Marston, J. O.; Chan, D. Y. C.; Thoroddsen, S. T. Stabilization of Leidenfrost vapour layer by textured superhydrophobic surfaces. *Nature* **2012**, *489*, 274−277.
(49) Li, F.; Du, M.; Zheng, Z.; Song, Y.; Zheng, Q. A Facile, Multifunctional, Transparent, and Superhydrophobic Coating Based on a Nanoscale Porous Structure Spontaneously Assembled from Branched Silica Nanoparticles. *Adv. Mater. Interfaces* **2015**, *2*, 1500201.
(50) Lv, D.; Zhu, M.; Jiang, Z.; Jiang, S.; Zhang, Q.; Xiong, R.; Huang, C. Green Electrospun Nanofibers and Their Application in Air Filtration. *Macromol. Mater. Eng.* **2018**, *303*, 1800336.
(51) Ma, W.; Li, W.; Liu, R.; Cao, M.; Zhao, X.; Gong, X. Carbon dots and AIE molecules for highly efficient tandem luminescent solar concentrators. *Chem. Commun.* **2019**, *55*, 7486−7489.
(52) Li, Z.; Zhao, X.; Huang, C.; Gong, X. Recent advances in green fabrication of luminescent solar concentrators using nontoxic quantum dots as fluorophores. *J. Mater. Chem. C* **2019**, *7*, 12373−12387.
(53) Shirtcliffe, N. J.; McHale, G.; Newton, M. I. The superhydrophobicity of polymer surfaces: Recent developments. *J. Polym. Sci. Pol. Phys.* **2011**, *49*, 1203−1217.
(54) Ding, Q.; Xu, X.; Yue, Y.; Mei, C.; Huang, C.; Jiang, S.; Wu, Q.; Han, J. Nanocellulose-Mediated Electroconductive Self-Healing Hydrogels with High Strength, Plasticity, Viscoelasticity, Stretchability, and Biocompatibility toward Multifunctional Applications. *ACS Appl. Mater. Interfaces* **2018**, *10*, 27987−28002.
(55) Gao, S.; Dong, X.; Huang, J.; Li, S.; Li, Y.; Chen, Z.; Lai, Y. Rational construction of highly transparent superhydrophobic coatings based on a non-particle, fluorine-free and water-rich system for versatile oil-water separation. *Chem. Eng. J.* **2018**, *333*, 621−629.
(56) Alawajji, R. A.; Kannarpady, G. K.; Biris, A. S. Fabrication of transparent superhydrophobic polytetrafluoroethylene coating. *Appl. Surf. Sci.* **2018**, *444*, 208−215.
(57) Wu, X.; Fu, Q.; Kumar, D.; Ho, J. W. C.; Kanhere, P.; Zhou, H.; Chen, Z. Mechanically robust superhydrophobic and superoleophobic coatings derived by sol-gel method. *Mater. Des.* **2016**, *89*, 1302−1309.

https://dx.doi.org/10.1021/acsomega.9b03775
ACS Omega 2020, 5, 4100−4108